Bachelor Thesis:

Investigating the effect of microfibre on the printability and strain hardening properties of Strain-Hardening Cement-based Composites(SHCC)

By

Daan Coppus

Commissioned by the course CTB3000, Bachelor of Civil Engineering

Delft University of Technology

Faculty of Civil Engineering and Geosciences

Research group: Materials & Environment

June 7, 2022

Thesis Supervisors: Ph.D. candidate (Anne Linde) van Overmeir

Dr. B. (Branko) Šavija

Preface

You are now reading my thesis that was written as part of the graduation of the bachelor's degree in civil engineering at Delft University of Technology. During 8 weeks I researched different concrete mixtures for the application of 3D printing of concrete. Through this research, I hope that the world in which 3D printing of concrete is a widely used application, will come a step closer.
While researching I was able to use the facilities of the faculty of civil engineering such as the Stevin Lab and the Microlab. I am very pleased that for the first time during my bachelor I have been able to do a practical concrete research in these labs.
This report is intended for anyone interested in the development of 3D concrete printing or microfibre reinforcement in concrete. Some prior knowledge of concrete properties and basic mechanics is necessary to understand this report.

I want to thank Anne Linde van Overmeir and Branko Šavija for introducing me to this topic and providing the guidance needed.

Daan Coppus

Delft, June 7, 2022

Summary

This report describes the effect of microfibre reinforcement on the printability and strain hardening properties of Strain-Hardening Cement-based Composites (SHCC). To determine this effect, a study was conducted with three different fibre types and two different concrete matrices. In total, this has led to 6 different concrete mixtures. The three different fibre types are PVA(Poly-Vinyl-Alcohol) 6mm length, PVA 8mm length and HDPE(High Density Poly Ethylene) 6mm length. The difference between the two matrices is mainly in the water-cement ratio, which leads to a stronger and weaker matrix. The strong matrix is the C mix and the weaker one is the D mix.

The printability of the different mixtures is determined by means of a slump flow test. Printability can be divided into buildability and pumpability. Buildability describes how well the printed concrete layers hold together and do not collapse. Pumpability of the mixture says how well it is able to be pumped. If the slump flow test shows that a mixture behaves stiff, than it will have a higher buildability and lower pumpability. If the mixture behaves very fluidly in the slump flow test, it will have a lower buildability and higher pumpability.

The strain hardening properties of the SHCC are determined by doing compressive tests, four-point bending tests and tensile tests. These tests determine the compressive strength, flexural strength and tensile strength of each mixture. It was also found out to what extent each mixture is able to stretch, bend and then exhibits strain hardening. After the tests, the samples were also visually examined to see how the bending and cracking took place.

The weak D mix seems to show the most strain hardening. The fibres in this matrix can transfer the tensile stresses better, because in this matrix they are more able to stretch.

The research has shown that the mixtures with PVA 6 mm in the fresh state are very stiff and are therefore the least suitable for 3D printing. In addition, the mixtures with the PVA 6 mm microfibre reinforcement show the least strain hardening. In the four-point bending tests it was already noticeable that the samples failed at very low deflection and there was little cracking. It was therefore decided not to include these mixtures in the tensile tests in order to save time.

HDPE microfibre has shown to have good printability and significantly outperforms PVA 8 mm in strain hardening. The HDPE fibres provide a very flexible and stretchable material. Compared to PVA, HDPE shows a much finer cracking pattern, which has a positive effect on the durability of the concrete. All in all, it can be concluded that HDPE performs best and would be the best choice for application in 3D printing.

Table of Contents

1. Introduction

1.1 Background Information

3D concrete printing is a technology under development. Making a 3D-printed concrete structure works as follows: a 3D-concrete printing device pumps the mortar through a hose towards the nozzle and places the mortar in small layers on top of each other. The nozzle can deposit the mortar in almost any desired shape via a 3D-computer-controlled program. This 3D-printing technology offers the opportunity to enable not only rectangular but also organic forms of building, something that architects often find aesthetically pleasing. In addition, this technique also provides possibilities for applying the construction material only in the places where it is necessary from a structural point of view, the so called "form follows force" principle.

1.2 Problem Statement

Applying classic steel reinforcing bars in 3D-printed structures is impractical. As an alternative to traditional reinforcement Strain-Hardening Cement-based Composites (SHCC) is used for the application of 3D-printed concrete structures. These SHCC consist of a mortar mixture to which microfibres are added, which serve as reinforcement. As soon as SHCC is loaded above a certain stress, called the matrix cracking strength, microcracks will appear in the concrete. The microfibres in the SHCC will now start taking over the tensile forces and show strain-hardening characteristics.

Figure 1: Principle of strain hardening ((Muzenski, Vivian, Sobolev, & Mechtcherine, 2016)

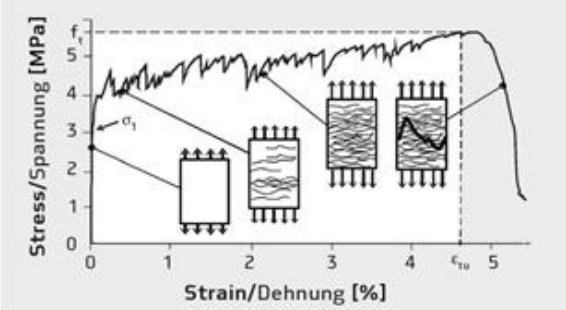

The challenge of applying SHCC lies in the fact that the material must not only be printable in the fresh state, but also has to meet the hardened properties to ensure strain hardening capacity.
The printability can be divided into pumpability and buildability. First of all, the pumpability is important for the processing of the SHCC. Since the SHCC must be able to be pumped through a hose towards the nozzle, it must not get stuck in the pump nor in the hose or nozzle. The SHCC must also be easy to clean from the printing device after use. Furthermore the entire pumping process should not cost too much energy.
In addition to pumpability, buildability also plays a role in printability. Buildability describes the resistance of the fresh material to deform under a certain load. For good buildability, it is therefore important that the printed layers remain properly aligned and that the deformation of the lower layers due to gravitational loading is limited.
From literature it is found that the amount and type of microfibres in the SHCC will not only affect the strain hardening properties of the material but also the printability. (Ogura, Nerella, & Mechtcherine, 2018)

This research will investigate the effect of microfibre on the printability and the strain hardening properties of Strain-Hardening Cement-based Composites(SHCC).

1.3 Objectives and Research Question

Main research question

What is the effect of microfibre on the printability and the strain hardening properties of Strain-Hardening Cement-based Composites(SHCC)?

Objectives

1. Determining the effect of different microfibre types on the fresh properties of Strain-Hardening Cement-based Composites.
2. Determining the effect of different microfibre types on strain hardening properties of Strain-Hardening Cement-based Composites

1.4 Project Description

Two different types of microfibres are used for this research: PVA (Poly-Vinyl-Alcohol) and HDPE (High Density Poly Ethylene). For the PVA fibre lengths of 8 mm and 6 mm will be used and for HDPE only 6 mm fiber length will be used. In addition to the differences in fiber length between the PVA 8 mm and PVA 6 mm microfibres, there is a difference in diameter as well. Furthermore there is small difference in E modulus.

Table 1: Microfibre properties

	PVA - 8 mm	***PVA – 6 mm***	***HDPE – 6 mm***
Tensile strength [MPa]	*1600*	*1600*	*3000*
Modulus of elasticity [Gpa]	*42.5*	*37*	*80*
Ultimate strain [%]	*6*	*6*	*3.5*
Length [mm]	*8*	*6*	*6*
Diameter [µm]	*39*	*26*	*20*
Aspect ratio [L/D]	*205*	*231*	*300*

In order to investigate the effect of different microfibre types on the printability and the strain hardening properties of SHCC, tests will be executed with six different SHCC mixtures.
To evaluate the printability of the SHCC with different fiber types, a slump flow test will be done. In this test, the fresh SHCC is placed in an open cone, after which the cone is lifted and the diameter with which the fresh SHCC flows out is measured. The table top will then be dropped 15 times, after which the diameter of the material will be measured again.

At 14 and 28 days after casting the SHCC samples, the strain hardening properties of the different mixtures are tested.

A compressive test will be performed. Cubes with 40 mm edges will be made from the different mixtures. The forces, cracks and deformation during this test will be monitored.
In addition a four-point bending test will be performed, in which the sample is fixed at both ends and the sample will be loaded at 1/3 of span ends so that the bending moment distribution will be constant in the middle of the sample. This test will also be a displacement-controlled test.
A tensile test will be carried out at 28 days strength only. In the tensile tests, the samples are loaded in the longitudinal direction by means of a displacement-controlled test. During this test, a constant displacement is used, whereby the forces and crack formation of the samples are monitored until the moment the sample fails.

1.5 Limitations and Preconditions

Only 8 weeks have been set aside for this bachelor's final project. Time is therefore the biggest limiting factor during this research. Prior to the practical research, a “startnotitie” had to be made and a safety briefing had to be followed. As a result, the practical part of this study could not begin until the beginning of week 3. Bearing in mind that the strain hardened properties of the concrete must be measured up to 28 days after casting, it lets this project push the boundaries of the schedule.
In view of the high time pressure, only the influence of the different microfibers can be taken into account and only three different microfibers are tested, PVA 8 mm, PVA 6 mm and HDPE 6 mm. Those microfibres are tested combined with 2 matrix designs called Mix C and Mix D. Thus a total of 6 mixes will be investigated in this research.
In addition, only the slump flow test, compressive test, four-point bending test and tensile test can be carried out. Doing other additional tests does not fit within the timeframe of this project.

2. Theory

2.1 SHCC theory

Strain-Hardening Cement based Composites(SHCC), derives its name from its strain hardening properties in the hardened state when loaded. Unlike traditional standard concrete structures that use steel reinforcing bars, SHCC uses microfibre self-reinforcement. When the SHCC is loaded under tension and the matrix cracking stress is exceeded, microcracks will be formed. Due to the incorporation of microfibres as self-reinforcement, the SHCC sample will not fail in a brittle way. Depending on the bond between the fibre and the cementitious matrix, the fibre could be able to bridge the microcrack and restore the force equilibrium. From literature it was found that: "*The interaction between the cementitious matrix and the fibre is essential for obtaining a SHCC with strain hardening properties."* (Overmeir, et al, 2022) If the fibre is able to bridge the microcrack the load could be increased, subsequently new microcracks will be formed and then these microcracks can be bridged by other fibres. This process of bridging multiple microcracks by microfibres leads to a material with high ductility which is characterizing for SHCC.

2.2 Four-point bending, beam theory

Figure 2: mechanics four-point bending

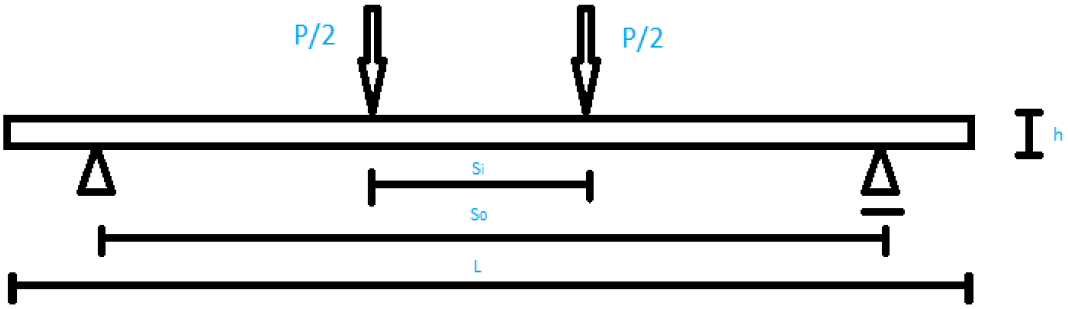

Parameters :

$$Si = \frac{S0}{3} = 40\ mm$$

$$S0 = 120\ mm$$

$$L = 150\ mm$$

Figure 3: V-line four-point bending

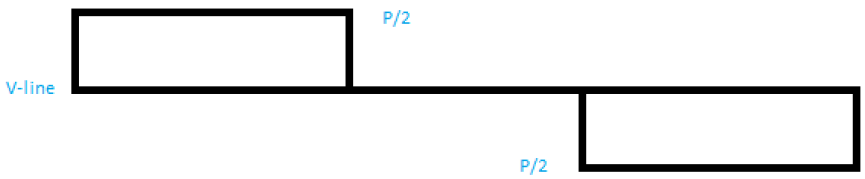

Figure 4: M-line four-point bending

$$M = \frac{P * (S0 - Si)}{4} = \frac{\frac{2}{3}S0 * P}{4} - \frac{1}{6}S0 * P$$

$$\sigma, \max = \sigma flex, \max = \frac{-M * y}{I} = \frac{\left(\frac{-1}{6} * S0 * P\right) * (-\frac{1}{2}h)}{\frac{1}{12} * b * h^3} = \frac{\frac{1}{12} * So * P * h}{\frac{1}{12} * b * h^3} = \frac{So * P}{b * h^2}$$

2.3 Tensile theory

Figure 5: tensile test mechanics

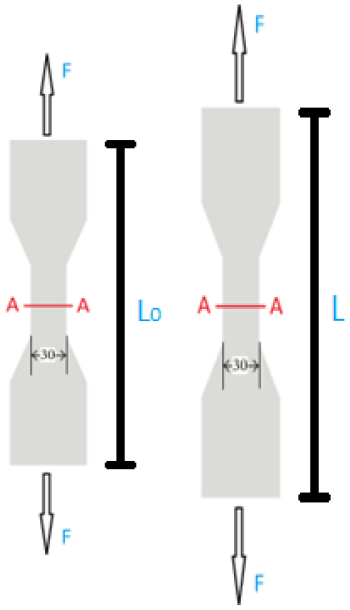

$$\sigma = \frac{F}{A}$$

$$\varepsilon = \frac{\Delta L}{L0} = \frac{L - L0}{L0}$$

3. Material

A quantity of 3.5 liters of each mixture is required to make the SHCC samples and perform all test within this research. *Table 2* indicates the composition of each mixture.

Table 2: composition mixtures

TOTAL VOLUME = 3.5 LITER	Mix C + PVA 6 mm	Mix C + PVA 8 mm	Mix C + HDPE 6 mm	Mix D + PVA 6 mm	Mix D + PVA 8 mm	Mix D + HDPE 6 mm
BFS – eco2cem [gram]	951.69	951.69	951.69	919.95	919.95	919.95
cem 1 42,5 [gram]	1703.25	1703.25	1703.25	1646.44	1646.44	1646.44
Silica Fume [gram]	119.23	119.23	119.23	115.25	115.25	115.25
Limestone Inducal 105 [gram]	2114.15	2114.15	2114.15	2043.64	2043.64	2043.64
Sand 125-250 [gram]	1149.69	1149.69	1149.69	1111.35	1111.35	1111.35
Water [gram]	1328.36	1328.36	1328.36	1400.79	1400.79	1400.79
VMA [gram]	12.48	12.48	12.48	10.73	10.73	10.73
Super Plasticizer [gram]	11.10	11.10	11.10	9.39	9.39	9.39
PVA 6 mm [gram]	91.00	0	0	91.00		0
PVA 8 mm [gram]	0	91.00	0	0	91.00	0
HDPE [gram]	0	0	68.25	0	0	68.25

The mixing of the ingredients must be done according to a prescribed procedure. The mixing procedure (Overmeir, et al, 2022) is described below:

- *2 Minutes: Mixing all dry materials, including fibres, super plasticizer and* $\frac{1}{3}$ *of the VMA*
- *1 Minute: Adding of water while mixing*
- *1 Minute: Mixing of wet material*
- *Add:* $\frac{2}{3}$ *of the VMA*
- *2 Minutes: Mixing of wet material*

4. Test methodology

4.1 Slump flow test methodology

The slump flow test is performed according to the standard in ASTM C230/230 M. In this test the fresh SHCC is poured into a conical cylinder. The dimensions of the conical cylinder: 50 mm high, 70 mm top diameter and 100 mm bottom diameter. After the cylinder has been filled, it is pulled up and the fresh concrete mixture remains on the flow table. The slump is then determined by measuring the difference in height between the cylinder and the concrete mix. Subsequently the fresh concrete mixture undergoes an impact loading by the collision of the flow table to the bottom stand. The flow table drops through a constant height of 12.7 mm for 15 times at a constant rate. (Cho, et al., 2020) Next, the mean diameter of the fresh concrete mixture is measured. This is done by taking the average of the diameter in two orthogonal directions of the fresh concrete mix. (See figures below for illustration) The above steps are repeated every 5 minutes until the moment the fresh concrete mixture has an age of 30 minutes after completion of the mix procedure.

Figure 6: illustration impact loading (Cho, et al., 2020)

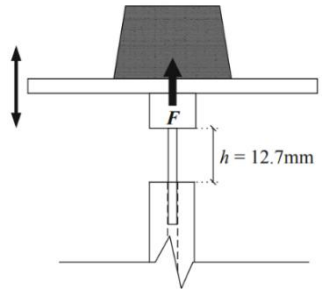

Figure 7: test set up

Figure 8: determine slump

Figure 9: determine flow after 15 table drops

Figure 10: determine orthoganal diameters

$$d = \frac{Dy + Dx}{2}$$

4.2 Compressive test methodology

The SHCC is casted in prismatic beams. After the prismatic beam has partially cured, blocks of 40 x 40 x 40 mm are sawn from the beam. The compressive test is performed 14 and 28 days after casting of the samples. All test samples have been cured at 20 ◦C with a relative humidity of 97% prior to testing. In this compressive test, an increasing compressive force will be applied to the sample until it fails. The test was conducted in a servo hydraulic machine with a constant load rate of 2 kN/s in accordance with ASTM C-39. (C39/C39M-17, 2017) To prevent unevenness during the test on the sides of the test blocks, it is important to place the sawn sides of the blocks up and down in the servo hydraulic machine. The moment the test sample fails, the machine will display the force at which this happened.

To arrive at a reliable conclusion, at least four samples must be tested to determine the mean and the standard deviation of the compressive strength.

Figure 11: compressive test set up

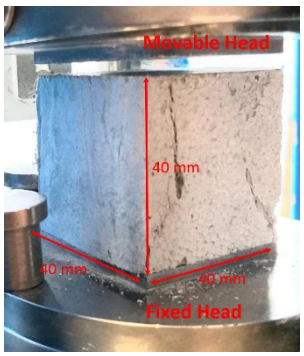

4.3 Four-point bending test methodology

The four-point bending test is performed to determine the flexural strength of the SHCC samples. This test is performed on samples of 14 and 28 days old, with dimensions of 30 mm * 7 mm * 150 mm. The samples have been cured at 20 ◦C with a relative humidity of 97% prior to testing.

The samples are placed in an Instron 8872 servo-hydraulic machine, which then initiates a displacement-controlled test of 0.01 mm/s. The span of the test sample is 120 mm with the two metal rods exerting a force 40 mm apart. See *Figure 2* for a schematic view. The testing system measures what force is needed to make the sample displace 0.01mm/s at the roller positions. The mean displacement of the rollers is measured by means of two LVDTs.

Figure 12: four-point bending test set up

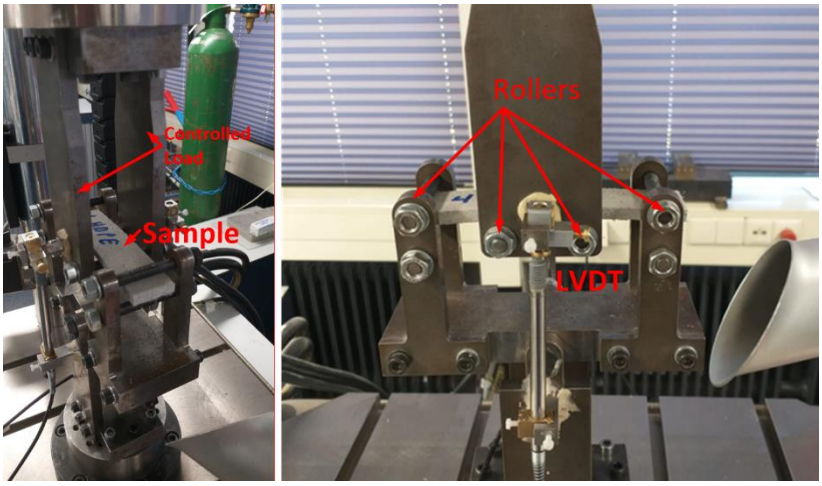

4.4 Tensile test methodology

To perform the tensile test, the SHCC is casted in a so-called dogbone mold. The samples have been cured at 20 ◦C with a relative humidity of 97% prior to testing . The dimensions of the dogbone mold are shown in *Figure 13*. The shape of the dogbone ensures that failure will occur in the region of smallest cross-section. The test samples are only tested for their 28 day strength in this test. Using the

Instron 8872 servo-hydraulic machine, a deformation-controlled test will be performed with a displacement speed of 0.005 mm⁄s. The vertical displacement of the sample is measured by means of two LVDTs. The tensile samples are glued to the testing machine with glue.

Figure 13: dimensions dogbone sample (Bang, Prabhu, Jang, & Kim, 2015)

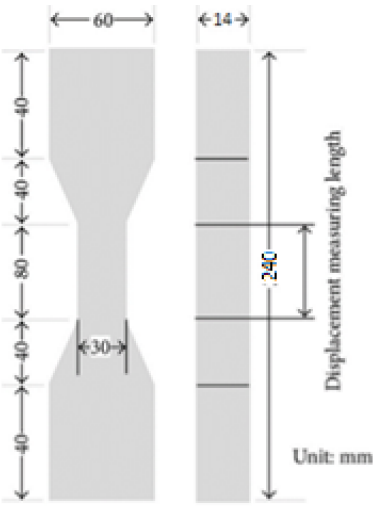

Figure 14: tensile test set up

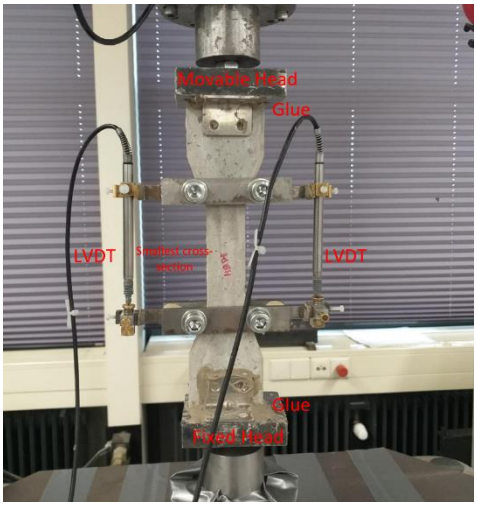

5 Results and Analysis

5.1 Slump flow test and printability analysis

After every 5 minutes the mean slump and the mean flow of the fresh SHCC were determined. These results can be found in *Appendix A.* In order to evaluate the printability of each different SHCC mixture, only the flow will be taken into account. In *Figure 15* the results of the mean diameter, after every 15 table drops, of the fresh SHCC are plotted. During the slump flow test the samples, that will be used during the tests to determine the strain hardening properties, were casted. As a result, due to time constraints, no measurements were taken for the mixtures C + PVA 8 mm, C + HDPE and D PVA 6 mm at the time when the fresh SHCC was 10 minutes old.

Figure 15: plotted results flow test

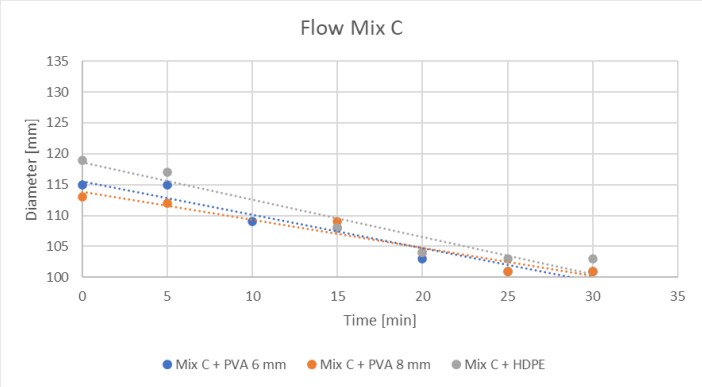

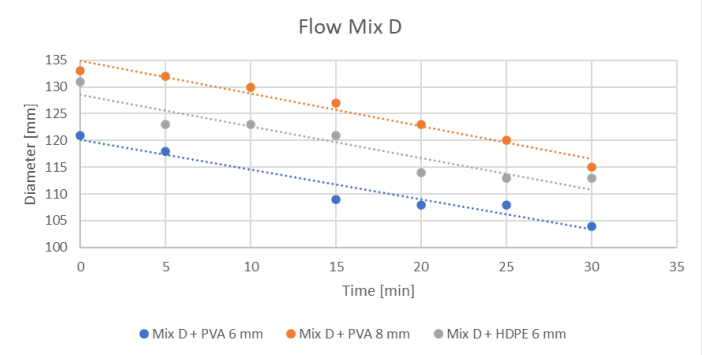

The stiffer the mixture, the higher the buildability of the printing layers of the material. Downside of this is that stiffer material has a lower pumpability. From the above results it can be concluded that mix D shows a larger flow and therefore has a lower buildability but a better pumpability than mix C. Mix D has a higher water content than mix C, which means that this mixture has a lower viscosity and is therefore more pumpable. This is in line with the theory from *Figueiredo, et al. (2019)* that noted that *"a higher volume of water in the solution changes significantly the flowability of mixtures"*.
Fibre types PVA 6 mm and HDPE have the smallest diameters, 26 µm and 20 µm respectivly, see *Table 1*. All fibre types are added at an equal volume, thus the smaller the fibre diameter the larger the total effective area of the fibres. Whenever the effective area of the fibres is larger and the fibre material is hydrophilic, the SHCC mixture is more able to absorb water into the fibres. As a consequence, less water is available to the mortar itself, making the mixture stiffer in the fresh state. If the water content

in a mixture is larger, this effect is enhanced. This phenomenon can therefore be observed very strongly in the flow tests of mix D, as the water content in these mixtures is larger.
Although the diameter of the PVA 6 mm fibres is slightly larger than the HDPE fibre diameter, the PVA 6 mm mix D shows a stiffer behaviour in the fresh state. This at first sight unexpected observation may be explained by the fact that HDPE is a hydrophobic material, which means that the absorbtion of water is less than with PVA (Abeysinghe, et al., 2021).

5.2 Compressive Test

The compressive test measurements, mean compressive strengths and standard deviations of the samples can be found in *Appendix B*. The mean compressive strengths are plotted in the bar chart below.

Figure 16: compressive strenght performance

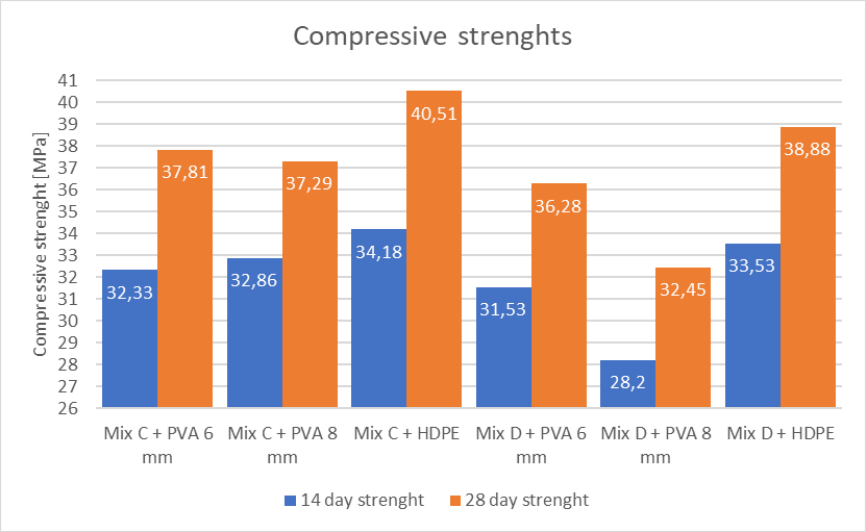

In general, it can be said that the C mixtures have a greater compressive strength than the D mixtures. This is a result that is within expectations. The C mix has a lower water content than the D mix, a lower water-cement ratio is thus created, which leads to a stronger concrete matrix. In addition, it can be seen that for each mix, the compressive strength after 28 days is higher than the 14 day compressive strength. This can be explained by the fact that the hydration reaction of the concrete making it stronger is in a further stage.
From the above results it can be observed that the compressive strength of the HDPE mixtures is somewhat higher than the PVA mixtures. This observation may be explained by the hydrophobic properties of the HDPE fibres. Due to the fact that the HDPE fibres are hydrophobic, a microstructure is formed that has a lower porosity and therefore a higher compressive strength. The PVA fibres, on the other hand, bind better to the water, so that voids could be formed between the matrix and the fibre. As a result the PVA mixtures will have a higher porosity and therefore a lower compressive strength.
As previously described in section 5.1, the PVA 6 mm fibres have a larger total effective area than the PVA 8 mm fibres. As a consequence more water can be absorbed into the PVA 6 mm fibres. Subsequently less water is available for the matrix itself, creating a lower water-cement ratio and therefore a higher compressive strength. It can be stated that: the higher the water content, the weaker the PVA 8 mm behaves compared to the PVA 6 mm. This is completely in line with the results

from *Figure 16.* In mix C the difference between PVA 6 mm and PVA 8 mm is significantly smaller than in mix D, as the water content of mix D is higher the absorbing effect is enhanced. When the results of the slump-flow test and the compressive test are compared, it can be noted that PVA 6 and 8 mm show approximately the same behavior in the C mix. However it can be seen that the values for the mix D differ.

5.3 Four-point bending test and flexural hardening analysis

The measurement results and associated graphs can be found in Appendix C. A representation of the mean flexural strengths and corresponding standard deviations is shown in *Table 3*. Due to lack of time and inexperience in casting procedures of concrete, some results show high standard deviations. Despite these large deviations, an attempt has been made to determine the bending performance and flexural hardening properties of the different mixtures.

Table 3: Results four-point bending test

	MIX C + PVA 6 MM	MIX C + PVA 8 MM	MIX C + HDPE	MIX D + PVA 6 MM	MIX D + PVA 8 MM	MIX D + HDPE
14 DAY FLEXURAL STRENGTH [MPA] (RELATIVE STDEV)	8,87 (11,27%)	8,18 (16,87%)	9,27 (10,68%)	8,41 (5,8%)	8,51 (14,22%)	9,30 (16,13%)
CORRESPONDIG DISPLACEMENT ROLLERS [MM] (RELATIVE STDEV)	4,74 (12,45%)	6,29 (17,01%)	8,99 (15,13%)	5,48 (29%)	12,38 (23,10%)	13,09 (13,52%)
28 DAY FLEXURAL STRENGTH [MPA] (RELATIVE STDEV)	12,97 (13,96%)	7,21 (17,20%)	9,48 (16,03%)	7,89 (29,02%)	9,18 (16,12%)	11,33 (13,32%)
CORRESPONDIG DISPLACEMENT ROLLERS [MM] (RELATIVE STDEV)	7,75 (33,16 %)	3,81 (31,50%)	7,49 (38,72%)	4,00 (52,25 %)	13,40 (17,16%)	12,49 (13,61%)

Figure 17: results four-point bending test

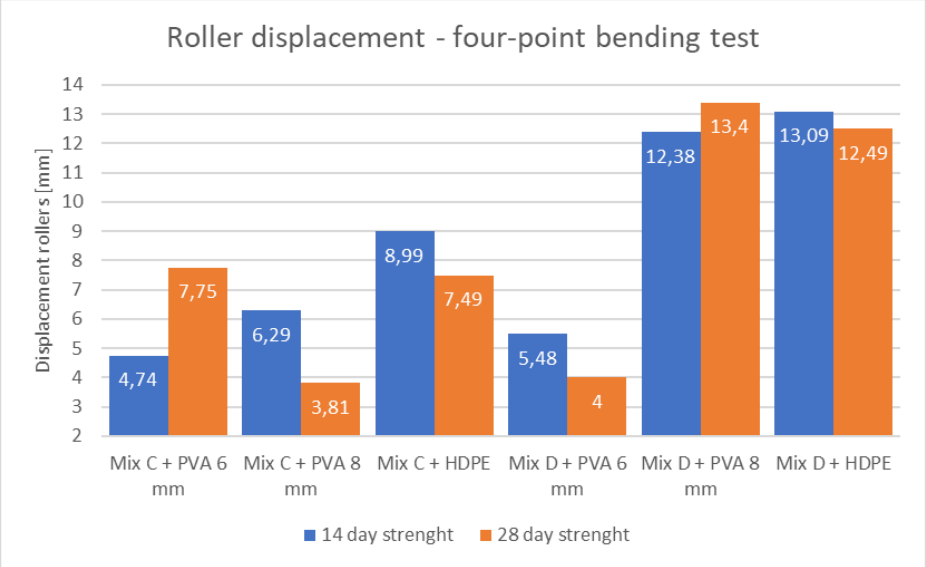

As can be seen in the figure above, the samples perform better on average during the 14-day test than during the 28-day test. This observation can be explained by the development of the matrix strength.

As the SHCC gets older, the matrix becomes stronger. If the matrix becomes stronger, there is less opportunity for the microfibres to stretch in the matrix and the fibers will fail sooner.
There is a significant difference found between the C and D mixtures as well. The D mix exhibits much more flexural hardening behavior than the C mix and can displace more. In this case the matrix strength is again the basis for this. Considering the higher water-cement ratio in mixture D, a weaker matrix is formed. This allows the microfibers to stretch more in the material, resulting in higher displacements.
The PVA 6 microfibre appears to do the worst and in comparison to the other fibre types. PVA 6 mm mixtures shows hardly any bendability and flexural hardening properties. Looking at the graphs in Appendix C, it is shown that the PVA 6 mm graphs have verry few drops. These drops, which are caused by cracking of the SHCC, are necessary for bridging the tensile stresses and in this way create strain hardening behavior.
HDPE on the other hand, performs very well in this test. The HDPE samples are able to bend very far and many drops can be seen in the graphs. After an optical inspection, it can also be seen that the HDPE fibers have a finer cracking pattern than the other fibers. This observation is consistent with the literature found earlier from *Ogura, Nerella & mechtcherine, (2018)* who stated that: "*SHCC with HDPE fiber show finer crack patterns for the same fiber content, which is beneficial with respect to durability and serviceability".* A finer cracking pattern ensures that water, salts and chemicals are less able to penetrate the concrete, so that it can serve longer.

Figure 18: HDPE vs PVA 6 mm

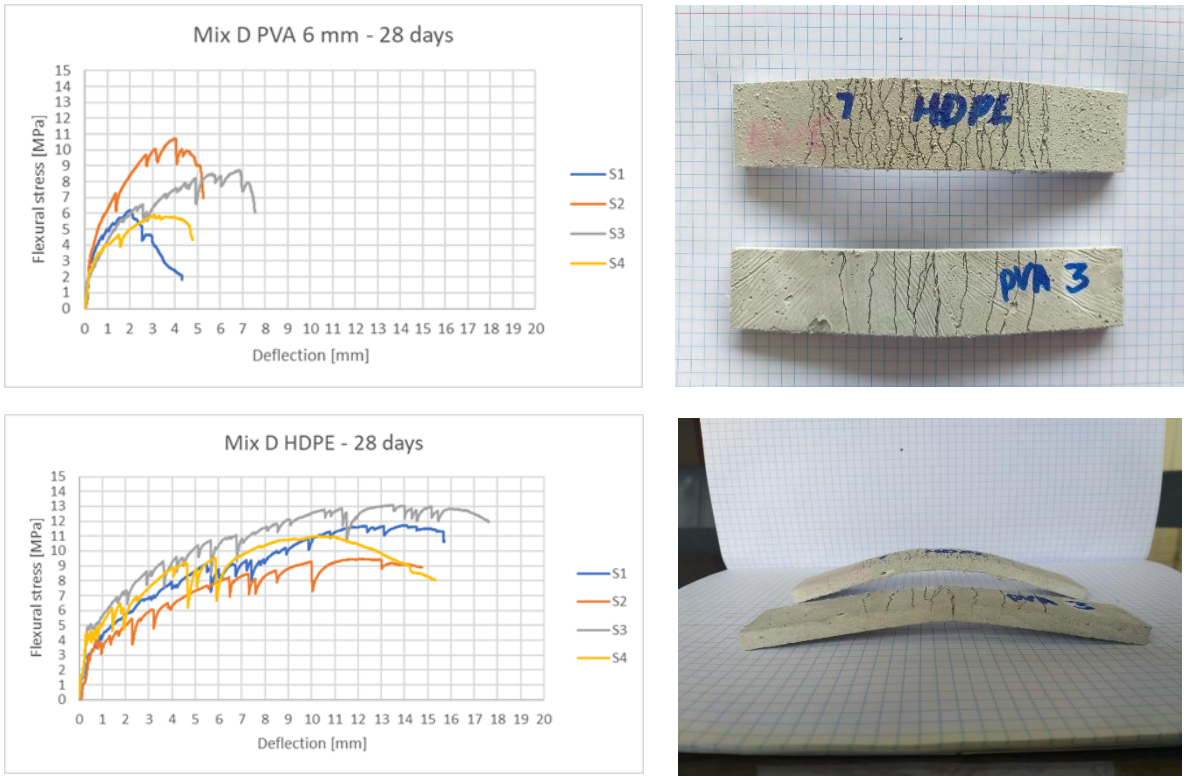

Figure 18 shows the difference between HDPE and PVA 6 mm fibres. The amount of drops in the graphs corresponds with the cracks formed. HDPE does not only generate more cracks and a finer cracking pattern but also a higher deflection.

5.4 Tensile test and strain hardening analysis

The results and graphs of the tensile test are shown in Appendix D. The PVA 6 mm is not included in these tests. Based on the four-point bending test and the slump flow test, PVA 6 mm has shown to have insufficient flexural bending capacity and to high initial stiffness for the application of 3D concrete printing. The material is too stiff and shows too little strain hardening properties. Due to lack of time and inexperience in casting procedures of concrete, some results show high standard deviations. Despite these large deviations, an attempt has been made to determine the tensile performance and strain hardening properties of the different mixtures.

Table 4: tensile test results

	MIX C + PVA 8 MM	MIX C + HDPE	MIX D + PVA 8 MM	MIX D + HDPE
28 DAY TENSILE STRENGTH [MPA] RELATIVE STDEV	3,99 (7,02%)	4,63 (7,99%)	4,63 (6,26%)	4,32 (10,65%)
CORRESPONDIG STRAIN [%] RELATIVE STDEV	0,87 (22,07%)	1,3 (20,0%)	2,1 (47,62%)	2,0 (55,0%)

In *Table 4* and *Figure 19* it is visible that the D mix outperforms the C mix. Again, the higher water-cement ratio creates a weaker matrix, which ensures that the microfibres can stretch better in the material. The high deviations of the D mix is most likely caused by the LVDTs being clamped to the sample. Because of this clamp attached to the sample, additional stresses may have arisen, causing the deviation to be higher. In addition it is very difficult to tighten the clamp in exactly the same way during each test. For the performance of the C mix, the LVDTs are glued to the sample. This prevents the occurrence of extra irregular stresses. This immediately shows a decrease in the standard deviation. Hence it is a lot more reliable to say something about the measurements with the C mix than those with the D mix.

Figure 19: stress-strain graphs

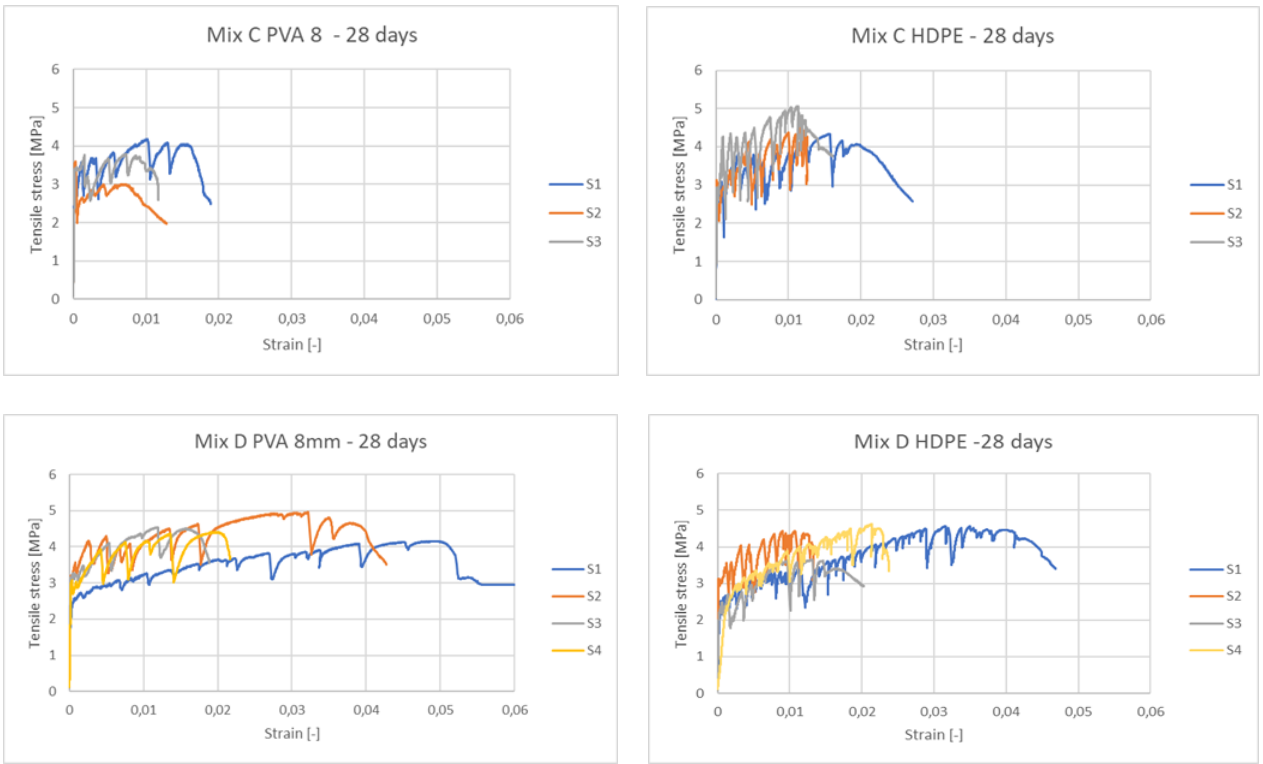

Considering only the C mix tests, it can be stated that HDPE requires more strain to fail than the PVA 8 mm microfibre. Just like the four-point bending tests, the number of drops in the graph clearly shows that the HDPE fibres form significantly more cracks. In addition, it can be seen that the failing cross-sections have a different character. (See figure below)

Figure 20: failing cross-section Mix C HDPE vs Mix C PVA 8 mm

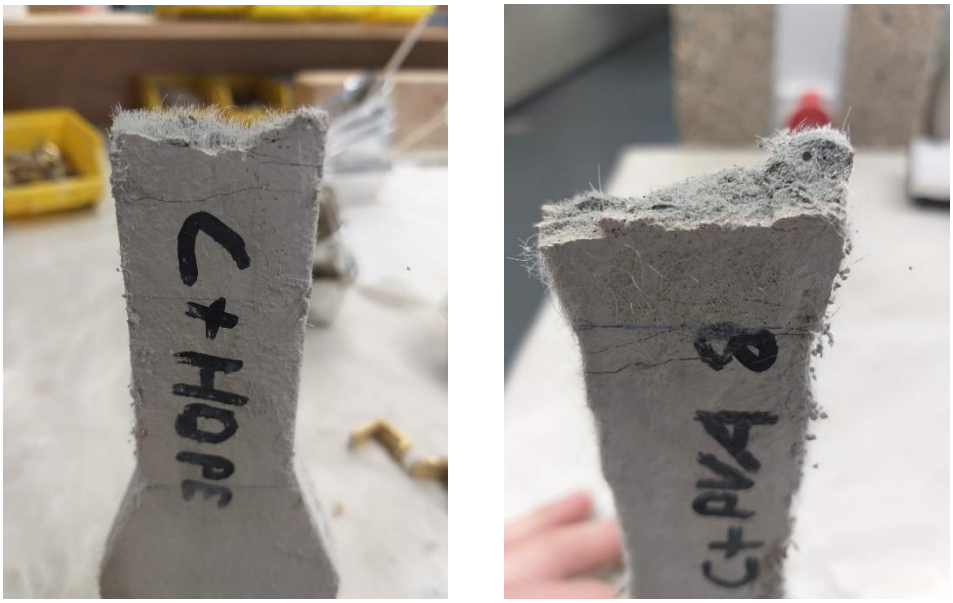

It can be seen in *Figure 20* that the microfibres inside the failing cross-section in the HDPE sample stick out more in comparison to the PVA 8 mm sample. The PVA 8 mm fibres mainly show breakage.

Discussion

As mentioned in chapter 1, time has been the biggest limiting factor in this study. In order to work as efficiently as possible, it was therefore decided to do the slump flow test and the casting of the samples at the same time. Due to inexperience and the great time pressure during this lab session, not all samples were casted in a proper way, see *Figure 21A* . This has resulted in a large standard deviations in some tests. In the compressive tests, this standard deviation has remained fairly limited. In the four-point bending tests and the tensile tests, on the other hand, an extremely high deviation of the results can be seen within some mixes.

With regard to the four-point bending test, there are some limitations to the test set-up. Firstly, in most results, a small irregularity can be seen in the linear elastic region of the stress-displacement diagram, see *Figure 21B*. This irregularity is caused by a small displacement of the rollers in the test set up. The rollers are not completely fixed in the test set up. The irregularity therefore arises because this is the moment when the roller moves up and then is fixated by the test set up. Secondly, it should be noted that the contact between the rollers and the samples is not completely frictionless and an additional stress is created. In theory, the largest deflection would occur in the middle of the samples and should therefore fail here as well. However, it has been found that the majority of the samples failed at the roller location.

Silicone molds were used for casting the tensile samples. Unfortunately, it turned out that some molds had been lying on a table that was not completely flat during curing. This resulted in some skewed samples, which may have influenced the reliability of the test.

Fixing the LVDTs on the samples was done by screwing a clamp. This clamp most likely created extra stresses in the material. As a result, some test results were unusable due to the sample not failing in the smallest cross-section, see *Figure 21C*. This happened with the D mix tests. For the C mixes it was decided to glue the LVDTs to the samples. This has solved the problem and reduced the standard deviation of the results as well.

Figure 21: points of attention for follow-up research

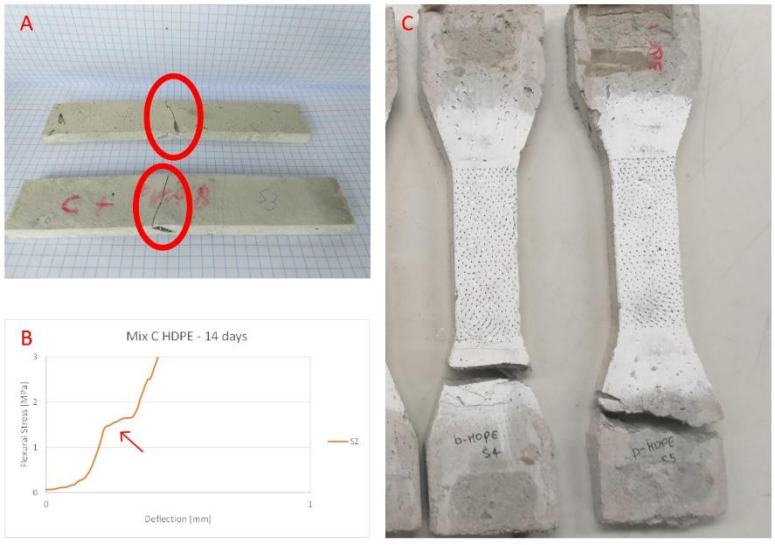

Conclusions

The main question to be answered in this research is: *What is the effect of microfibre on the printability and the strain hardening properties of Strain-Hardening Cement-based Composites(SHCC)?* The following can be concluded after conducting this research:

- The printability of the different mixtures was tested by means of the slump flow test. The following can be concluded with regard to the printability of the different mixtures:
  Mixes with the PVA 6 mm microfibre show the stiffest behaviour. This will ensure a low pumpability, making the PVA 6 mm less suitable for the application off 3D concrete printing. When the water-cement ratio is increased, this will have a positive effect on the pumpability of the mixture. The downside of this is that the buildability decreases. The HDPE and PVA 8 mm microfibre both score considerably better in terms of printability.

- The flexural and strain hardening properties of the different mixtures were determined by means of the four-point bending test and the tensile test. The following has emerged from this:
  PVA 6 mm showed the least flexural hardening. PVA 8 mm and HDPE did significantly better in flexural hardening. A notable difference between these two fibre types is that HDPE exhibits a finer cracking pattern with several smaller cracks. This fine cracking pattern has a positive effect on the durability and serviceability of the material. The HDPE fibres also show a better bendability than the PVA 8 mm fibres. Finally, it was noted that the mix with a higher water-cement ratio and thus the lowest matrix strength, exhibits more flexural and strain hardening than mixes with a lower water content. The fibres in these mixes are more able to stretch in the material.
  Based on the tensile test with the C mix, it can be concluded that the HDPE fibre exhibits more strain hardening. It is difficult to draw a conclusion about the D mix since there was an enormous standard deviation.

Taking into account what has been mentioned above, it can be concluded that the HDPE microfibre is most suitable for application in 3D printing of concrete. However, this conclusion can only be drawn for the mixtures used in this study. When different ingredients or a different composition of ingredients is used , the outcome may differ.

Recommendations for future research

For future follow-up research, it is recommended not to do the casting of the samples and testing of the fresh properties on the same day. Performing this simultaneously can result in great time pressure. This can lead to irregularities in the samples that could affect the test results. Moreover, it can ensure that fewer measurements can be made on the fresh properties.

Furthermore, the four-point bending test set up could be improved by using fixed rollers that cannot move. To get a correct observation of the linear elastic area in stress-strain or stress-displacement graphs, where the linear elastic part becomes a straight line without a kink in it. It would also be great if somehow the friction between the rollers and the samples could be reduced. Making the samples less likely to fail at the roller positions. The four-point bending test set up used in this study, has been developed in such a way that only the displacement of the rollers can be measured. It would be very interesting for some follow-up research to measure the displacement off mid-span position. Nevertheless this set up will require major adjustments to make room for an LVDT at mid-span position.

When using silicone molds in the future, it is strongly recommended to closely examine the flatness of the table. In this way the samples are prevented from taking a skewed shape when they are curing. To improve the quality of the tensile tests, it is beneficial to glue the LVDTs on the samples. This prevents additional stresses in the samples, as is the case with clamping the LVDTs to the samples.

This research has shown that the HDPE microfibre seems to be the most suitable for the application of 3D concrete printing. However, in this study no 3D concrete printers were used. All samples used during this research were casted. A possible follow-up study would therefore be to 3D print the HDPE samples and do the different tests again. It is then possible to investigate the properties of the SHCC when it is actually printed and to what extent these differ from the casted samples.

References

Abeysinghe, S., Gunasekara, C., Bandara, C., Nguyen, K., Dissanayake, R., & Mendis, P. (2021). *Engineering Performance of Concrete Incorporated with Recycled High-Density Polyethylene (HDPE)—A Systematic Review.* Switzerland: MDPI.

Bang, J. W., Prabhu, G. G., Jang, Y. I., & Kim, d. Y. (2015). *Development of Ecoefficient Engineered Cementitious Composites Using Supplementary Cementitious Materials as a Binder and Bottom Ash Aggregate as Fine Aggregate.* Cairo: Hindawi Publishing Corporation.

C39/C39M-17, A. (2017). *Standard Test Method for Compressive Strength of Cylindrical Concrete Specimens.* www.astm.org: ASTM International.

Cho, S., Kruger, J., Bester, F., Heever, M. v., Rooyen, A. v., & Zijl, G. v. (2020). *A Compendious Rheo-Mechanical Test for Printability Assessment of 3D Printable Concrete.* Paris: RILEM.

Figueiredo, S. C., Rodríguez, C. R., Ahmed, Z. Y., Bos, D., Xu, Y., Salet, T. M., . . . Bos, F. P. (2019). *An approach to develop printable strain hardening cementitious.* Netherlands: Elsevier.

Muzenski, S., Vivian, I. F., Sobolev, K., & Mechtcherine, V. (2016). *Hydrophobic and superhydrophobic strain-hardening cement-based composites. 82. 48-56.*

Ogura, H., Nerella, V. N., & Mechtcherine, V. (2018). *Developing and Testing of Strain-Hardening Cement-Based Composites (SHCC) in the Context of 3D-Printing.* Basel : MDPI.

Overmeir, A. L. (2022). *3D Printed Concrete: Self-reinforced concrete.* TU Delf - 3MD - Materials & Environment.

Overmeir, A. L., Figueiredo, S. C., Šavija, B., Bos, F. P., & Schlangen, E. (2022). *Design and analyses of printable strain hardening cementitious composites with optimized particle size distribution.* www.elsevier.com/locate/conbuildmat: Elsevier.

Appendix A – Results slump flow test

	Mix C + PVA 6 mm		Mix C + PVA 8 mm		Mix C + HDPE 6 mm		Mix D + PVA 6 mm		Mix D + PVA 8 mm		Mix D + HDPE 6 mm	
Time [min]	*Slump [mm]*	*Flow [mm]*	*Slump [mm]*	*Flow [mm]*	*Slump [mm]*	*Flow [mm]*	*Slump [mm]*	*Flow [mm]*	*Slump [mm]*	*Flow [mm]*	*Slump [mm]*	*Flow [mm]*
0	*10*	*115*	*10*	*113*	*11*	*119*	*13*	*121*	*15*	*133*	*18*	*131*
5	*10*	*115*	*10*	*112*	*11*	*117*	*8*	*118*	*14*	*132*	*14*	*123*
10	*8*	*109*							*13*	*130*	*13*	*123*
15	*5*	*108*	*8*	*109*	*6*	*108*	*3*	*109*	*12*	*127*	*8*	*121*
20	*1*	*103*	*2*	*104*	*2*	*104*	*2*	*108*	*8*	*123*	*6*	*114*
25	*1*	*101*	*2*	*101*	*1*	*103*	*2*	*108*	*6*	*120*	*5*	*113*
30	*1*	*101*	*1*	*101*	*1*	*103*	*1*	*104*	*6*	*115*	*4*	*113*

Appendix B – Results compressive test

Mix C + PVA 6mm - 14 days	
kN	*Mpa*
50,294	31,434
48,172	30,108
53,671	33,544
53,830	33,644
52,675	32,922
mean	**32,330**
stdev	**1,524 OR 4,71%**

Mix C + PVA 8mm - 14 days	
kN	*Mpa*
48,381	30,238
50,230	31,394
58,668	36,667
50,352	31,470
55,209	34,505
mean	**32,855**
stdev	**2,653 OR 8,08%**

Mix C + HDPE - 14 days	
kN	*Mpa*
49,465	30,916
57,009	35,630
54,890	34,306
56,383	35,240
55,688	34,805
mean	**34,179**
stdev	**1,900 OR 5,56%**

Mix D + PVA 6mm - 14 days	
kN	*Mpa*
51,534	32,209
51,444	32,152
51,112	31,945
45,903	28,690
52,401	32,651
mean	**31,529**
stdev	**1,608 OR 5,10%**

Mix D + PVA 8mm - 14 days	
kN	*Mpa*
46,320	28,950
43,889	27,437
46,023	28,765
41,888	26,18
47,454	29,659
mean	**28,198**
stdev	**1,385 OR 4,91%**

Mix D + HDPE - 14 days	
kN	*Mpa*
52,65	32,906
51,316	32,072
55,592	34,745
53,326	33,329
55,375	34,609
mean	**33,532**
stdev	**1,397 OR 3,40%**

Mix C + PVA 6mm - 28 days	
kN	*Mpa*
66,424	41,515
54,782	34,239
61,241	38,276
59,543	37,215
mean	**37,811**
stdev	**3,00 OR 7,93%**

Mix C + PVA 8mm - 28 days	
kN	*Mpa*
55,790	34,869
55,810	34,881
65,970	41,231
61,069	38,168
mean	**37,29**
stdev	**3,05 OR 8,18%**

Mix C + HDPE - 28 days	
kN	*Mpa*
65,230	40,769
66,557	41,598
67,317	42,073
60,181	37,613
mean	**40,51**
stdev	**2,01 OR 4,96%**

Mix D + PVA 6mm - 28 days	
kN	*Mpa*
52,944	33,090
60,009	37,505
57,877	36,173
61,343	38,339
mean	**36,28**
stdev	**2,30 OR 6,34%**

Mix D + PVA 8mm - 28 days	
kN	*Mpa*
53,736	33,585
50,116	31,323
52,810	33,006
50,990	31,869
mean	**32,446**
stdev	**1,034 OR 3,19%**

Mix D + HDPE - 28 days	
kN	*Mpa*
63,340	39,588
60,742	37,964
62,376	38,985
61,425	38,391
mean	**38,881**
stdev	**0,674 OR 1,73%**

	MIX C + PVA 6 MM	MIX C + PVA 8 MM	MIX C + HDPE	MIX D + PVA 6 MM	MIX D + PVA 8 MM	MIX D + HDPE
14 DAY COMPRESSIVE STRENGTH [MPA]	32,33 (4,71%)	32,86 (8,08%)	34,18 (5,56%)	31,53 (5,10%)	28,20 (4,91%)	33,53 (3,40%)
28 DAY COMPRESSIVE STRENGTH [MPA[	37,811 (7,93%)	37,29 (8,18%)	40,51 (4,96%)	36,28 (6,34%)	32,45 (3,19%)	38,88 (1,73 %)

Appendix C – Results four-point bending test

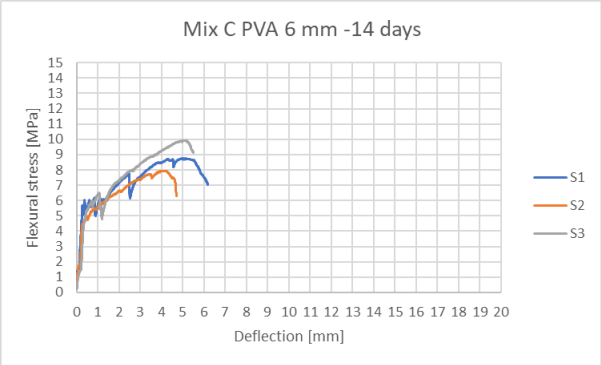

Sample	$\sigma_{flex,max}$ [MPa]	deflection at $\sigma_{flex,max}$ [mm]
S1	8,75	5,00
S2	7,94	4,07
S3	9,93	5,15
Mean	*8,87*	*4,74*
Standard Deviation	*1,00 OR 11,27%*	*0.59 OR 12,45%*

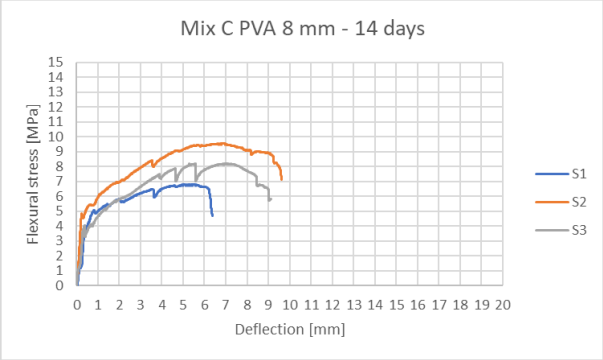

Sample	$\sigma_{flex,max}$ [MPa]	deflection at $\sigma_{flex,max}$ [mm]
S1	6,79	5,06
S2	9,55	6,82
S3	8,20	6,98
Mean	*8,18*	*6,29*
Standard Deviation	*1,38 OR 16,87%*	*1,07 OR 17,01%*

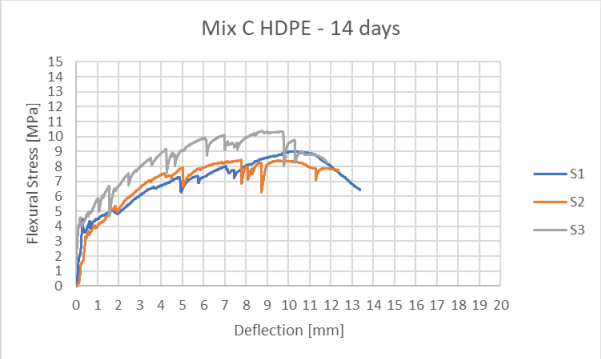

Sample	$\sigma_{flex,max}$ [MPa]	deflection at $\sigma_{flex,max}$ [mm]
S1	9,02	10,45
S2	8,43	7,77
S3	10,36	8,75
Mean	*9,27*	*8,99*
Standard Deviation	*0,99 OR 10,68%*	*1,36 OR 15,13%*

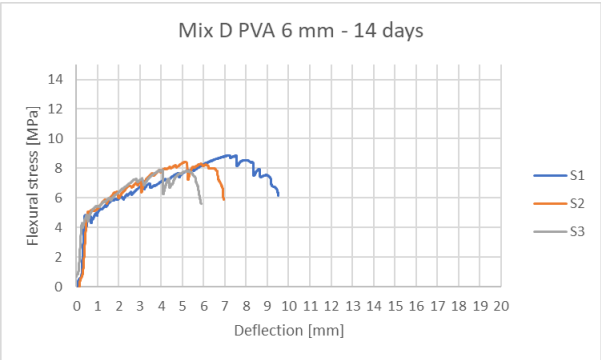

Sample	$\sigma_{flex,max}$ [MPa]	deflection at $\sigma_{flex,max}$ [mm]
S1	8,88	7,21
S2	8,45	5,16
S3	7,90	4,08
Mean	*8,41*	*5,48*
Standard Deviation	*0,49 OR 5,8%*	*1,59 OR 29%*

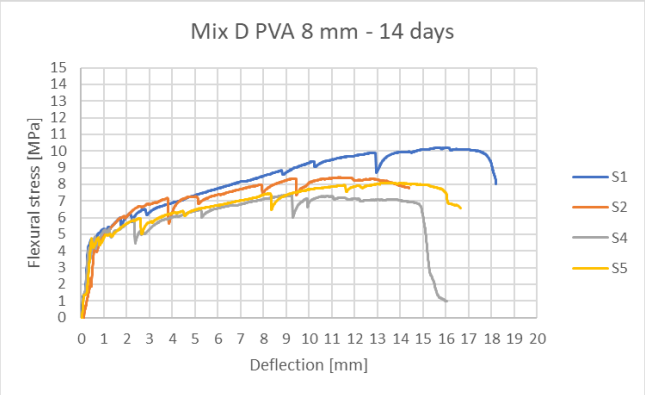

Sample	$\sigma_{flex,max}$ [MPa]	deflection at $\sigma_{flex,max}$ [mm]
S1	10,20	15,63
S2	8,41	11,27
S4	7,34	9,03
S5	8,09	13,59
Mean	*8,51*	*12,38*
Standard Deviation	*1,21 OR 14,22%*	*2,86 OR 23,10%*

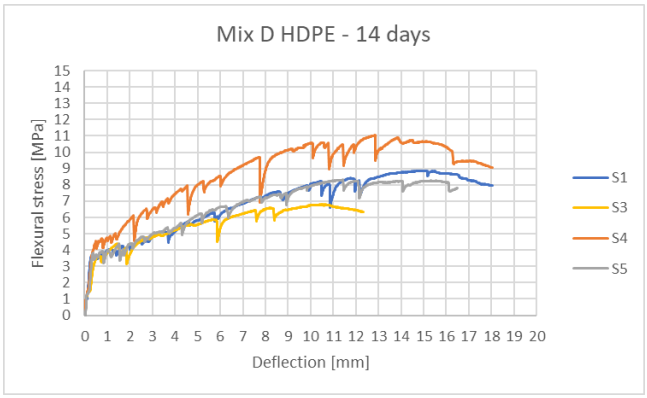

Sample	$\sigma_{flex,max}$ [MPa]	deflection at $\sigma_{flex,max}$ [mm]
S1	8,56	14,96
*S3**	6,79	10,52
S4	11,03	12,86
S5	8,31	11,44
Mean**	*9,30*	*13,09*
Standard Deviation**	*1,50 OR 16,13%*	*1,77 OR 13,52%*

*prestressed

**without S3

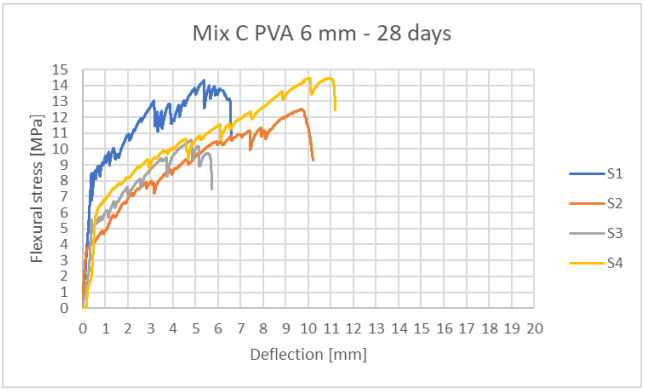

Sample	$\sigma_{flex,max}$ [MPa]	deflection at $\sigma_{flex,max}$ [mm]
S1	14,31	5,37
S2	12,51	9,70
S3	10,61	4,83
S4	14,46	10,10
Mean	*12,97*	*7,5*
Standard Deviation	*1,81 OR 13,96%*	*2,78 OR 37,07%*

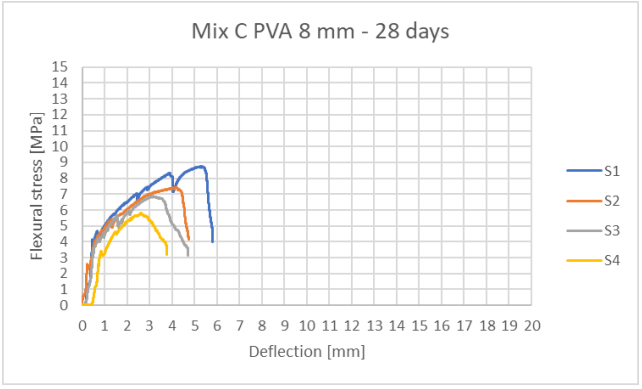

Sample	$\sigma_{flex,max}$ [MPa]	deflection at $\sigma_{flex,max}$ [mm]
S1	8,76	5,34
S2	7,42	4,14
S3	6,87	3,13
S4	5,79	2,62
Mean	*7,21*	*3,81*
Standard Deviation	*1,24 OR 17,20%*	*1,20 OR 31,50%*

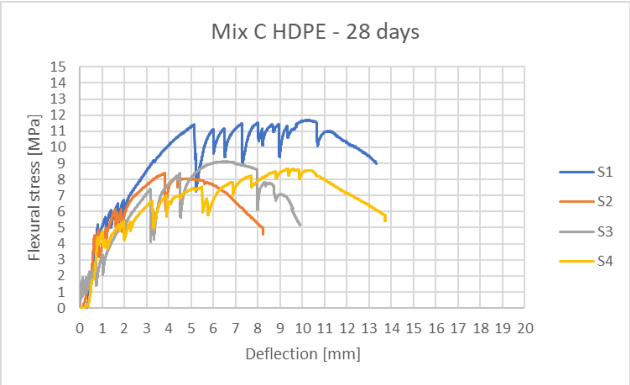

Sample	$\sigma_{flex,max}$ [MPa]	deflection at $\sigma_{flex,max}$ [mm]
S1	11,71	10,25
S2	8,39	3,82
S3	9,12	6,57
S4	8,69	9,31
Mean	*9,48*	*7,49*
Standard Deviation	*1,52 OR 16,03%*	*2,90 OR 38,72%*

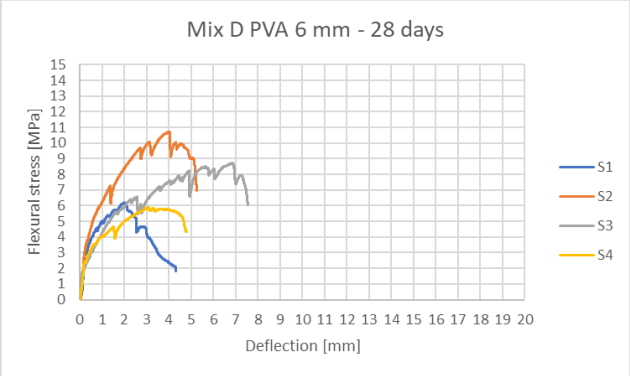

Sample	$\sigma_{flex,max}$ [MPa]	deflection at $\sigma_{flex,max}$ [mm]
S1	6,21	2,01
S2	10,73	4,03
S3	8,75	6,87
S4	5,88	3,08
Mean	*7,89*	*4,00*
Standard Deviation	*2,29 OR 29,02%*	*2,09 OR 52,25%*

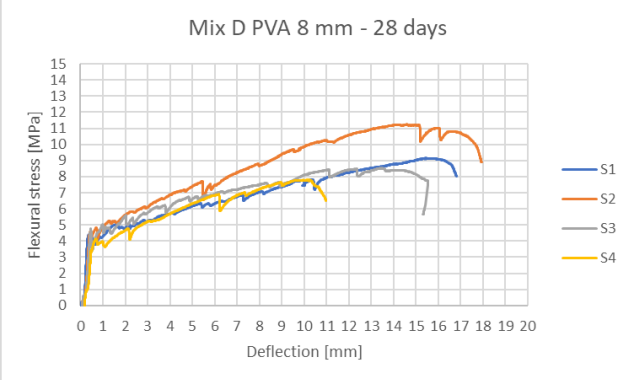

Sample	$\sigma_{flex,max}$ [MPa]	deflection at $\sigma_{flex,max}$ [mm]
S1	9,15	15,43
S2	11,24	14,58
S3	8,52	13,4
S4	7,80	10,19
Mean	*9,18*	*13,40*
Standard Deviation	*1,48 OR 16,12%*	*2,30 OR 17,16%*

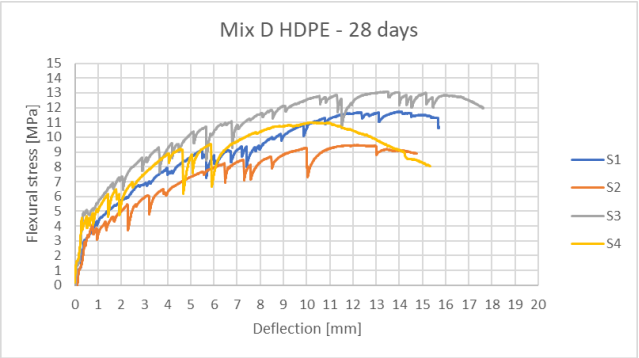

Sample	$\sigma_{flex,max}$ [MPa]	deflection at $\sigma_{flex,max}$ [mm]
S1	11,75	14,07
S2	9,47	12,15
S3	13,09	13,49
S4	11,01	10,24
Mean	*11,33*	*12,49*
Standard Deviation	*1,51 OR 13,32%*	*1,70 OR 13,61%*

Appendix D – Results tensile test

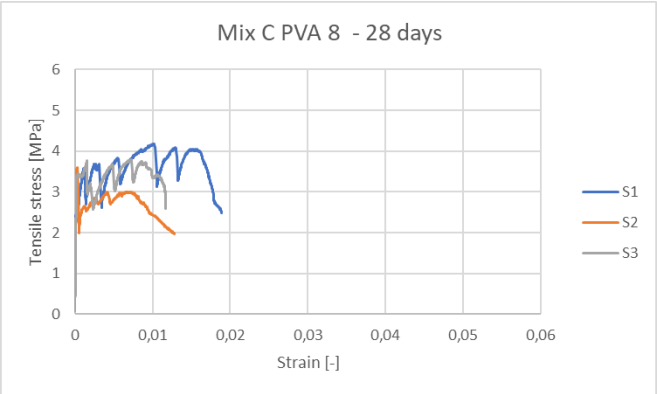

Sample	$\sigma_{ten,max}$ [MPa]	strain at $\sigma_{ten,max}$ [%]
S1	4,19	1,0
S2	3,60	0,0024
S3	3,79	0,73
Mean*	*3,99*	*0,87*
Standard Deviation*	*0,28 OR 7,02%*	*0,19 OR 22,07%*

*without S2

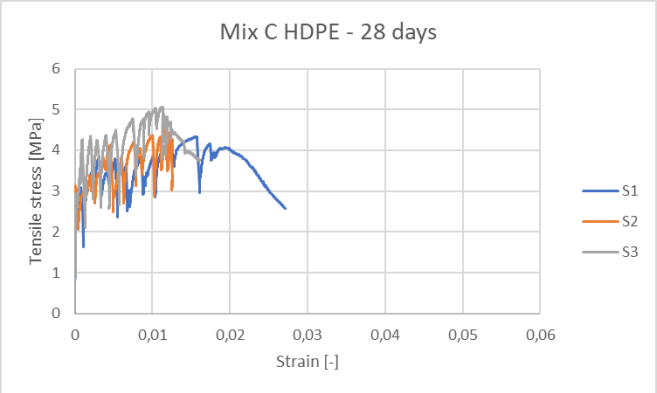

Sample	$\sigma_{ten,max}$ [MPa]	strain at $\sigma_{ten,max}$ [%]
S1	4,34	1,6
S2	4,51	1,2
S3	5,05	1,1
Mean	*4,63*	*1,3*
Standard Deviation	*0,37 OR 7,99%*	*0,26 OR 20,0%*

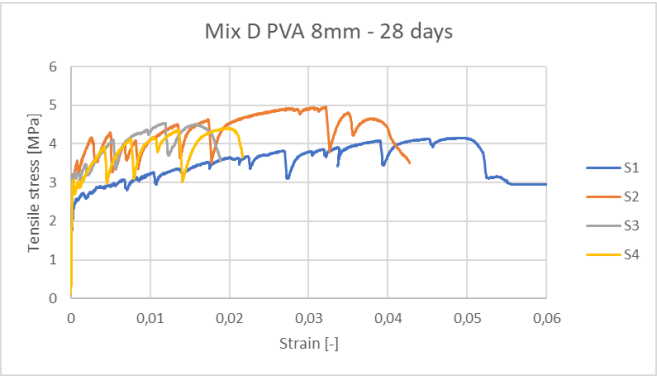

Sample	$\sigma_{ten,max}$ [MPa]	strain at $\sigma_{ten,max}$ [%]
S1	4,16	4,9
S2	4,96	3,2
S3	4,53	1,2
S4	*4,41*	*2,0*
Mean	*4,63*	*2,1*
Standard Deviation	*0,29 OR 6,26%*	*1,0 OR 47,62%*

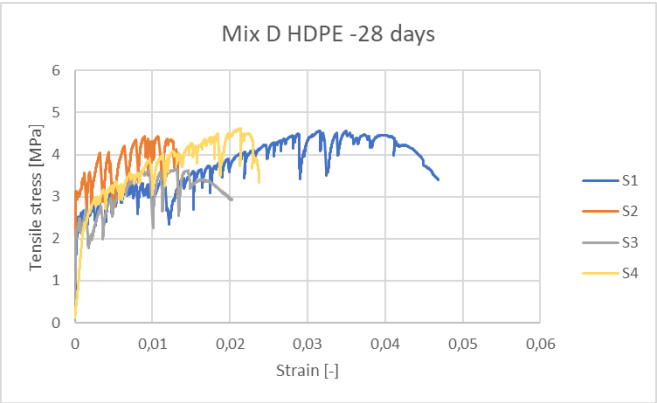

Sample	$\sigma_{ten,max}$ [MPa]	strain at $\sigma_{ten,max}$ [%]
S1	4,571	3,5
S2	4,44	1,1
S3	3,645	1,3
S4	4,63	2,1
Mean	*4,32*	*2,0*
Standard Deviation	*0,46 OR 10,65%*	*1,1 OR 55,0%*